



Radiation Copolymerization of PVA/Malic acid/ HEMA / Macroalgal (*Sargassum* sp.) Biomass for Removal of Hexavalent Chromium



Tarek Mansour Mohammed^{1,*}, Ahmed Labena², Nabila Ahmed Maziad¹, Shima Husien³

¹Polymer Chemistry Department, National Center for Radiation Research and Technology, Atomic Energy Authority, Cairo, Egypt P.O.Box 29, Nasr city. Cairo, Egypt.

²Biotechnology Laboratory, Processes Development, Egyptian Petroleum Research Institute (EPRI), Nasr City, Cairo, Egypt. P.O.Box 11727, Nasr city. Cairo, Egypt, Fax: (+202)22747433 Tel: (+202)26707519

³Environmental Science and Industrial Development, Faculty of Postgraduate Studies for Advanced Sciences, Beni-Suef University, Beni-Suef, Egypt.

BROWN macro-algal species (Seaweeds) biomass was collected and treated mechanically to reduce its size, increase its surface area and to polymerize easily with other polymer in a sheet. Polymerized algal cells in the polymer sheet have many advantages such as facilitate harvesting of the biomass in addition to enhanced heavy metals removal, recover from the industrial wastewater and the possibility to reuse application. Co-polymer-sheet of polyvinyl alcohol/ maleic acid/2- hydroxyethyl methacrylate/ Macroalgal biomass (PVA/ MAA /HEMA/ MacAlg) was successfully polymerized using Gamma ray technique. The prepared copolymer sheets were characterized with FT-IR, SEM, XRD and successfully applied to remove hexavalent chromium (VI) from contaminated water. One Factor at a Time (OFAT) experiments were studied for the polymer algal sheets to get the high and the low level that can further used in the Full Factorial Design optimization method. Chromium removal efficiency of 98.4 % was achieved at a concentration of 100 ppm after 3 h contact time. Isotherm and kinetics have been studied.

Keywords: Chromium (VI), Gamma radiation, Polyvinyl Alcohol, Maleic acid, 2- hydroxyethyl methacrylate, *Sargassum dentifolium*.

Introduction

The aquatic environmental - chromium contamination was induced by many industries effluents such as iron and steel industries, metal finishing industry, inorganic chemicals production and tanneries...etc [1]. Water contamination with high concentrations of chromium causes many hazardous effects on the environment [2]. Hexavalent chromium [Cr (IV)] considered as a mutagenic and carcinogenic material and most toxic form of chromium compounds [3]. It has

many hazardous effects on human health such as liver and lung cancer, kidney and gastric damage, sensitization and epidermal irritation [4]. Several conventional treatment approaches were applied for the Cr removal from contaminated wastewater as precipitation, reduction, solvent extraction and ion exchange [5,6]. However, these methods are ineffective especially at low concentrations of pollutants and showed high energy operation cost [7,8]. Therefore, searching for a new non-conventional method depending on biosorption is highly required. Biosorption is the process of

*Corresponding author email: tarekmmm75@yahoo.com; tarek.mansour@eaea.org.eg

Received 30/7/2019; Accepted 16/10/2019

DOI: 10.21608/ejchem.2019.15385.1936

©2020 National Information and Documentation Center (NIDOC)

accumulation and concentration of pollutants or heavy metals by using biomass [9,10]. Agriculture wastes and microbial organisms such as Fungi, bacteria and algae have been applied such as adsorbent materials for the removal and recovery of chromium from industrial waste water [11-14]. Different algal species such as *Chlorella vulgaris*, *Scenedesmus acutus*, *Sargassum* sp, *Ulva lactuca* were used for Chromium removal [15-18]. Advantages of using algae as a biosorbent material are attributed to its low cost and can be used in further purposes such as biogas, biodiesel and biofuel production and bio-fertilizers [19-21]. However, harvesting and dewatering of algal biomass from water after treatment considered a major challenge of algal biosorption processes. Therefore, polymerization of algal biomass in a polymeric material is a great idea for easy harvesting of algae and increases their removal efficiency [22]. The objective of this study was directed to use of *Sargassum dentifolium* with high surface area, by grinning and milling to relatively lowest size, polymerized in (PVA/MAA/HEMA) to form polymer algal sheet (PAS). After that PAS was used for hexavalent chromium [Cr (VI)] removal and was compared with other forms such as polymer alone and algal cell alone. OFAT experiments were used as preliminary experiments to determine the low and the high level of each factor. Full factorial design experiment was performed to obtain the optimum conditions that maximize the chromium removal efficiency [23]. The PAS was characterized using FT-IR spectroscopy, XRD and SEM. Moreover, isotherm and kinetics were studied.

Materials and Methods

Chemicals

Maleic acid and 2-hydroxyethyl methacrylate (HEMA) monomers of purity 99%, Potassium dichromate $K_2Cr_2O_7$ and polyvinyl alcohol PVA M wt. 89,000 were purchased from (Sigma-Aldrich, USA) and were used as received. Different concentrations of Cr (VI) were prepared by dissolving weighted amount of potassium dichromate $K_2Cr_2O_7$ in dist. water. Diphenyl carbazide was used for Cr (VI) estimation using spectroscopy technique.

Preparing of biosorbent material

Sargassum dentifolium, a genus of brown macro-algae (Class *Phaeophyceae*), as a biosorbent material was collected from Ras Gharb, Red Sea, Egypt. The algal biomass was washed with dist. water and dried in an oven at 50

°C for (~24h). After that the biomass was grinded by ball milling to achieve micro-size (Planetary Ball Mill PM 400 “4 grinding stations”) [24].

Polymer algal sheets (PAS) preparation

In 200 ml beaker a 0.5 gm of maleic acid was dissolved in 45 ml distilled water and 5 ml of HEMA was added to the beaker. Afterwards, a 50 ml of 8 % poly vinyl alcohol (PVA) was added to the solution with continuous steering. After that, the solution was subjected to gamma ray at 5 kGy (Dose rate 1.36407 kGy/h) to be converted to milky solution (Oligimar), then different weights of biomass were added to the solution with steering, and poured in clear Petri dishes and let sheets to dry at 37 °C.

Characterization of the polymer algal sheets (PAS)

FT-IR analysis

FT-IR spectra were used to state the functional groups of PAS. FT-IR spectra of the PAS were demonstrated using Attenuated total reflectance-Fourier transform infrared (ATR-FTIR) “Vertex 70 FTIR spectrometer” equipped with HYPERION™ series Microscope (Bruker Optik GmbH, Ettlingen, Germany), where definite amount of the sheet sample was mixed and grounded with KBr to form in pellets shape. IR spectra studies were detected at wavelength (400 – 4000 nm).

Scanning Electron Microscope (SEM) analysis

The SEM analysis, Jeol JSM-5400, was used to investigate the surface shape and the morphology of the PAS.

X-Ray diffraction analysis

The XRD-6000 series, Shimadzu apparatus using nickel filter and Cu-Ka target, Shimadzu Scientific Instruments (SSI), Kyoto, Japan was used in this study.

Effect of biomass dose

This experiment was used to determine the appropriate dose of biomass that can be loaded in the PAS. Different biomass doses (0, 0.1, 0.2, and 0.3) were investigated.

Batch adsorption experiment (OFAT experiments)

The batch adsorption studies were carried out in a 250 ml flask at room temperature. Experiments were conducted for different initial concentrations of Cr (VI) (100, 200, 300, 400, 500, 600 mg/l) and different pH values (3, 5, 7, 8 and 11). The flasks were placed in an orbital shaker with continuous shaking of 100 rpm at room temperature.

Moreover, the blank and the PAS were investigated in order to compare their efficiency with other forms. Cr (VI) was determined by using 721-spectrophotometer (M-MARKETAL) according to diphenyl carbazide method.

Cr (VI) removal efficiency (CRE) was calculated by the following equation:

$$\text{CRE (\%)} = \frac{C_0 - C_e}{C_0} \times 100 \quad \dots\dots (1)$$

OFAT experiments were investigated in order to determine the high (+) and the low (-) levels of factorial design.

Factorial design

The high (+) and the low (-) levels were defined to be used in the 2⁴ factorial designs as listed in Table (1). Selection of the high and the low levels of each factor was performed according to some preliminary experiments which presented above in

the batch adsorbent experiment. The full factorial design matrix, the CRE, fits and residuals were recorded for every run (see Table 2). The results were analyzed by Minitab-18 software, the main and the interaction effects, pareto chart and response optimizer of each factor were determined.

Desorption study

Desorption experiments were carried out for recovery and reuse of the PAS. Adsorption experiments of the PAS at conditions of an initial chromium concentration of 100 ppm, pH 7 and 25 ± 1 ° C. Afterwards, desorption process was obtained using 0.1M (EDTA, HCl, NaOH and HNO₃). At the end, the final chromium concentration was determined. After each adsorption – desorption cycle, the PAS washed with dist. water and used again.

Desorption ratio was calculated according to the following equation:

$$\text{Desorption ratio} = \frac{\text{amount of Cr. (VI) ions desorped to the desorption medium}}{\text{amount of Cr. (VI) ions adsorped onto polymer sheet.}} \times 100 \quad \dots(2)$$

Equilibrium isotherm studies

In order to determine the mechanism of sorption of Cr (VI) into the PAS, the linear form of Langmuir and freundlich isotherm was studied

Langmuir isotherm

Langmuir sorption model is designed to estimate the maximum Cr (VI) biosorption process using polymer algal sheets. The Langmuir isotherm expressed through the following equation:

$$\frac{C_e}{Q_e} = \frac{C_e}{Q_{\max}} + \frac{1}{b \times Q_{\max}} \quad \dots\dots(3)$$

Where q_e is the amount of metal ion sobbed (mg/g), b , represents a constant related to the adsorption/desorption capacity, and q_{\max} is the

maximum biosorption capacity upon complete saturation of the surface.

Freundlich isotherm

It's an empirical equation that used for the estimation of the adsorption intensity of the sorbent towards the adsorbent particles.

The following equation expresses the freundlich equation:

$$\log Q_e = \log KF + \frac{1}{n} \log C_e \quad \dots\dots(4)$$

Where q_e is the density of adsorption (where mg of the metal adsorbed/g biomass); C_e is the concentration of metal in the solution at equilibrium detected by (mg/L); KF and n are the Freundlich constants.

TABLE 1. high and low levels of the full factorial design experiment.

Factor	Unit	Symbol	Values of coded levels	
			-1 (Low)	+1 (High)
Contact Time-shaking model	h	CTS	1	3
Temperature	°C	Temp.	25	50
Chromium Concentration	ppm	Cr Conc.	100	500
Biosorbent material Quantity	-	BM	Algae	Blank
			Blank	PAS

Blank: polymer substance without algae, Sheet: immobilized algae in polymer, PAS: polymer algal sheet.

TABLE 2. The design matrix and the results of the 2⁵ full factorial design for BM.

Run Order	Cr (VI) conc.	AM	Temperature	Time	CRE	FITS1	RESI1
1	600	Blank	25	3	23.54846	29.88999	-6.341528
2	100	Algae	25	1	82.34313	66.08838	16.25476
3	600	Algae	50	1	19.8355	24.27173	-4.436225
4	100	Blank	25	1	59.25627	59.4159	-0.159629
5	100	Blank	50	1	59.57553	59.4159	0.159629
6	600	Sheet	50	3	54.59888	56.86731	-2.268429
7	600	Blank	50	3	36.23151	29.88999	6.341528
8	600	Algae	25	1	28.70795	24.27173	4.436225
9	100	Blank	50	3	67.01456	63.32781	3.686753
10	600	Algae	25	3	86.52074	74.08232	12.43842
11	100	Algae	50	3	97.77003	84.47726	13.29278
12	100	Algae	50	1	49.83362	66.08838	-16.25476
13	600	Sheet	25	3	59.13574	56.86731	2.268429
14	100	Algae	25	3	71.18448	84.47726	-13.29278
15	600	Blank	50	1	94.28848	83.85602	10.43246
16	100	Sheet	25	1	84.26704	79.04037	5.226665
17	600	Sheet	25	1	57.5482	47.91117	9.637031
18	100	Blank	25	3	59.64105	63.32781	-3.686753
19	600	Algae	50	3	61.6439	74.08232	-12.43842
20	100	Sheet	50	1	73.81371	79.04037	-5.226665
21	100	Sheet	50	3	98.41752	97.49877	0.918745
22	600	Sheet	50	1	38.27414	47.91117	-9.637031
23	100	Sheet	25	3	96.58003	97.49877	-0.918745
24	600	Blank	25	1	73.42357	83.85602	-10.43246

Sorption kinetics

The kinetics of biosorption process described the Cr (VI) ions adsorption by PAS and afforded useful information about the adsorption efficiency mechanism and the feasibility of scale-up operations. Pseudo 1st order and pseudo 2nd order models were used to analyze the kinetics of the sorption process.

Results and Discussion

Characterization of the polymer algal sheets (PAS)

FT-IR analysis

The co-polymerization and the function groups of PVA/ MAA /HEMA, PVA/MAA-HEMA/ polymer algal sheets were confirmed by FT-IR spectra. Results reported in the FT-IR spectrum of PVA/ MAA /HEMA, were shown (Fig 1a). The peak at 3383 cm⁻¹ was corresponded to the stretching O- H vibrations and the sharp band at 1247 cm⁻¹ is due to O-H bending vibrations [25]. A band at 1710 cm⁻¹ was corresponded to C=O stretching of the carboxylic groups of polymer, and the band observed at 1447 cm⁻¹ was due to CH₂ bending. Furthermore, the band at 2930 cm⁻¹ was attributed to stretching vibrations of C-H groups. The bands at 1395, 1247, and 1154 cm⁻¹

were originated from C- C, C- O, C-H bending vibration, respectively. Fig 1 b showed the FTIR of PVA/MAA-HEMA/ *Sargassum dentifolium*. Results reported a new peak at 2656 cm⁻¹ was attributed to NH group. Moreover, the peak at 1164 cm⁻¹ was attributed to C-N stretching vibrations. Fig 1c exhibited the FTIR spectrum of PVA/MAA-HEMA/*Sargassum dentifolium* that with adsorbed Cr (VI). Moreover, a new peak was appeared at around 1618, 1441 cm⁻¹ which was due to coupling between Metal-O and Metal-N, respectively.

Scanning Electron Microscope (SEM) analysis

SEM is “a type of microscope that produces image of sample by scanning the surface with a focused beam electrons. The electrons interact with atom in the sample producing various signals that contain information about the surface topography and composition of the sample”. Results reported in Fig 2a showed the SEM image that related to the PVA/MAA/HEMA/*Sargassum dentifolium* which were characterized by fine and smooth surfaces. After adsorption of chromium on the PAS, the SEM displayed images (see Fig 2 b) the Cr (VI) metal distribution and incorporation within the polymer sheet matrix in comparison to the surface before chromium uptake [23].

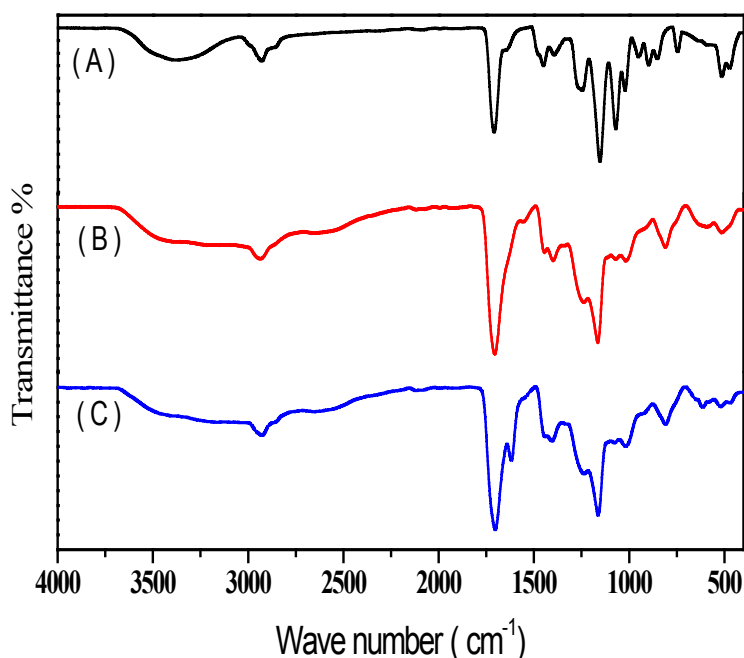


Fig.1. FTIR spectra of (a) PVA/ MAA /HEMA, (b) PVA/MAA/Sargassum and (c) PVA/MAA/HEMA/Sargassum//Metal.

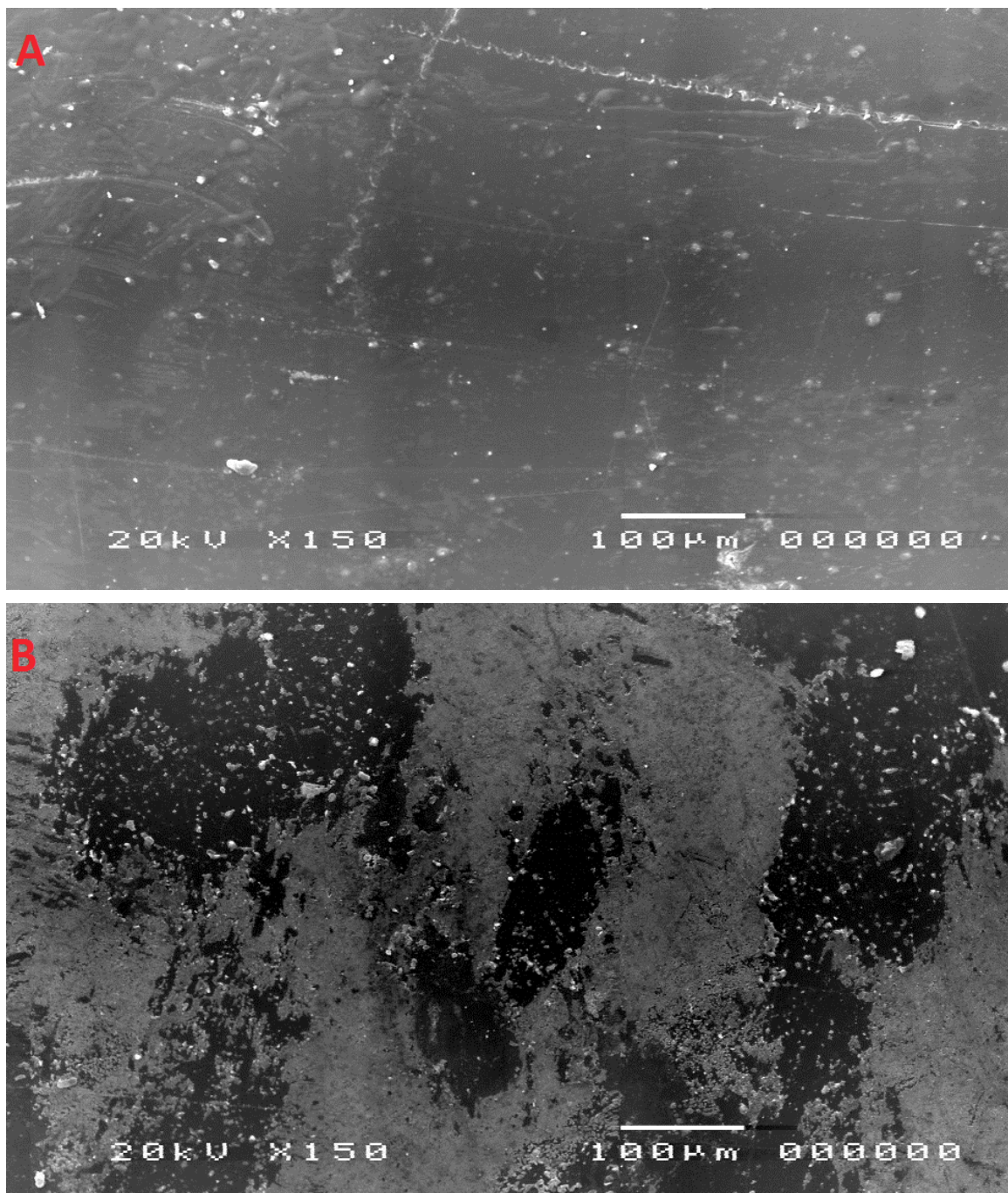


Fig. 2 SEM Images of the (PVA-MAA-HEAMA) and SEM of PVA/MAA-HEMA/Sargassumdentifolium/Metal.

X-ray Diffraction analysis

The XRD pattern displayed three characteristic peaks at $2\theta = 16.82^\circ$, 17.36° and 18.18° which indicated the crystallinity of PVA/MAA/HEMA film Fig 3. Fig 3 represented the indexed XRD pattern of PVA/MAA/HEMA which were corresponded to $2\theta = 31.33^\circ$, 31.67° and 36.19° , respectively. These results indicated the formation of highly crystalline PVA/

MAA/HEMA, PVA/MAA-HEMA/PAS. Fig 3 exhibited the XRD pattern, the presence of peaks at 2θ values 4.22° , 20.76° , and 20.35° , indicated the introducing of chromium ions within the polymer matrix which led to decreasing the crystallinity of the polymer sheet. This means that the amorphous phase of the polymer sheet was enhanced with introducing the chromium ions to the polymer matrix.

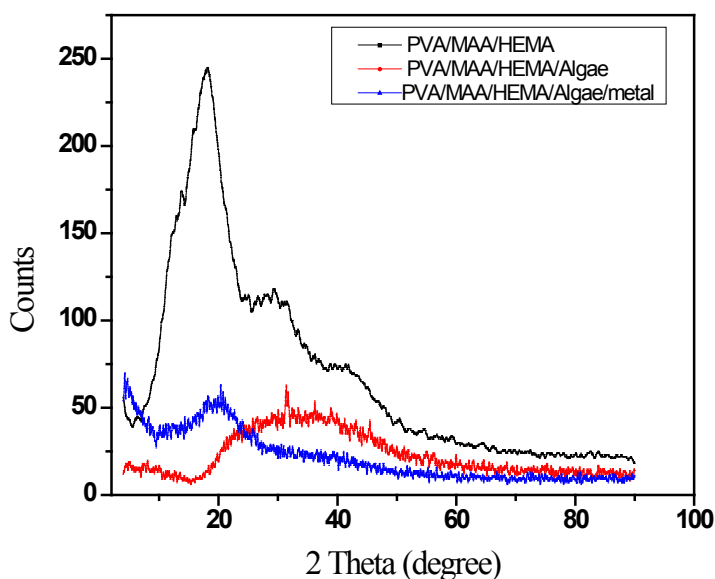


Fig. 3 . XRD pattern of polymer, polymer-algae and polymer-algae-metal.

Effect of immobilized Sargassum dentifolium dose

Data represented in Fig 4 reported that the 0.3 g of biosorbent material was the optimum algal dose that achieves the highest CRE in the PAS.

Full Factorial design

The factors that influence the CRE were demonstrated using factorial plots: main effects, interaction effects, pareto chart and response optimizer. ANOVA, student's t-test and the P-value express the significant levels and it was used in order to know the significance effect of the CRE. The main, the interaction effects, ANOVA, student's t-test were explained as follow:

The Main effects

The main effect of the factor is "defined as the change in the response that produced by the change in the level of one factor". The regression co-efficient and the main standard errors were displayed in Table 3 where the main effects (Time, Adsorbent type and Cr.(VI) conc.) represent deviation of the average of the high and the low level of each factor. The main effect plot illustrates only the factors that were significant with 95% confidence interval. It was noticed that, the Cr (VI) concentration has a negative effect on the CRE due to the reduction occurred from the low to the high level (see Fig 5). Moreover, the time has a positive effect due to the increase in the CRE from the low to the high level. Furthermore,

it should point out that the larger the vertical line between the high and the low level of the main factor, the larger the statistical significance. Therefore, it is easy to notice the great effect of the time on the CRE due to the larger vertical line between the high and the low level.

Interaction effect

The interaction is very effective when the change in the response from the low to the high levels of a factor depends on the level of the second factor. It means the lines of the two factors don't run parallel. Fig 6 showed the significant interaction between the factors (adsorbent type, time and Cr (VI) concentration). Those plots of interactions clearly indicated that the interaction between the adsorbent type and the time was the strongest interaction followed by interaction between the adsorbent type and the Cr (VI) concentration. The interaction between the Cr (VI) concentration and the time was statistically significant but much smaller. The effect of the adsorbent type and the Cr. (VI) concentration was more significant at low Cr (VI) concentration. Unlike the effect of adsorbent type and the time were more significant at the high level of time. The interaction effects between the adsorbent type & the Cr. (VI) concentration, adsorbent type& time and the Cr (VI) concentration and the time proved that the CRE were higher with the PAS at low Cr (VI) and high time.

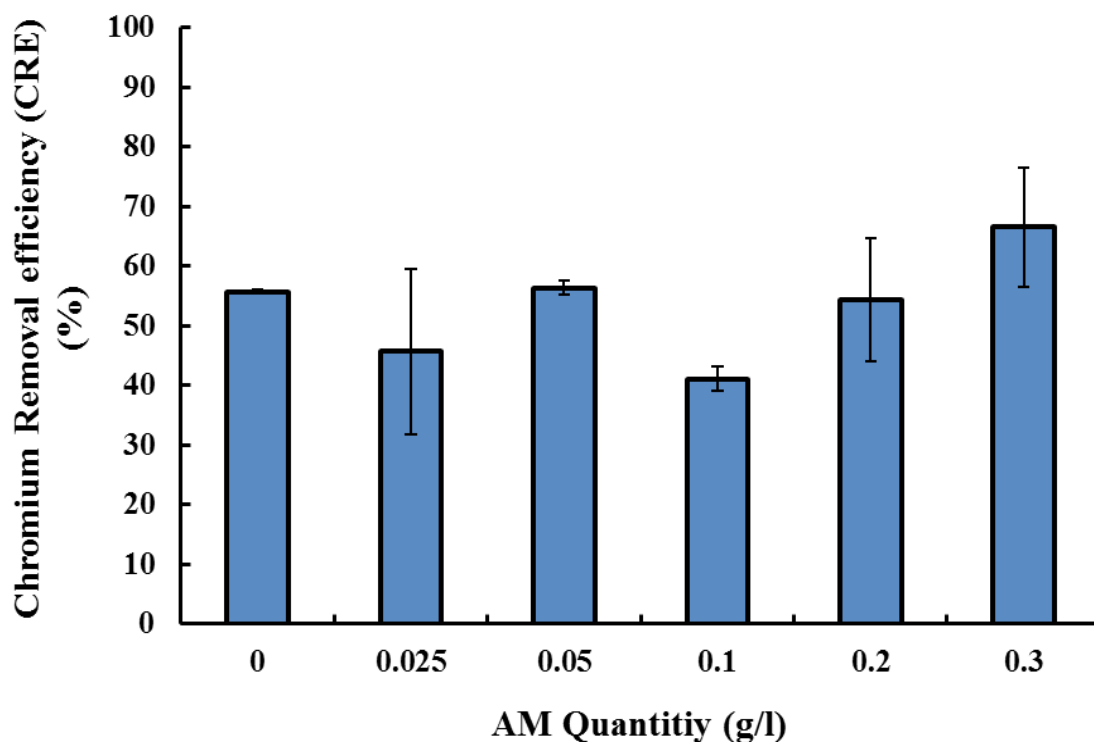


Fig.4 .The CRE at 100 mg/l initial chromium conc. with different *Sargassumdentifolium* conc. in the PAS.

TABLE 3. Estimated effects and coefficients for the CRE (%) of the BM.

Term	Coef	SE Coef	T-Value	P-Value	VIF
Constant	63.89	2.51	25.50	0.000	
Cr.(VI) conc.					
100	11.08	2.51	4.42	0.001	1.00
Adsorb. Type					
Algae	-1.66	3.54	-0.47	0.647	1.33
Blank	-4.77	3.54	-1.35	0.203	1.33
Time					
1	-3.80	2.51	-1.52	0.156	1.00
Cr (VI) conc.*Adsorb. type					
100 Algae	1.97	3.54	0.56	0.588	1.33
100 Blank	-8.83	3.54	-2.49	0.028	1.33
Cr.(VI) conc.*Time					
100 1	-3.00	2.51	-1.20	0.255	1.00
Adsorb. type*Time					
Algae 1	-13.25	3.54	-3.74	0.003	1.33
Blank 1	16.31	3.54	4.60	0.001	1.33
Cr.(VI) conc.*Adsorb. type*Time					
100 Algae 1	10.85	3.54	3.06	0.010	1.33
100 Blank 1	-11.47	3.54	-3.24	0.007	1.33

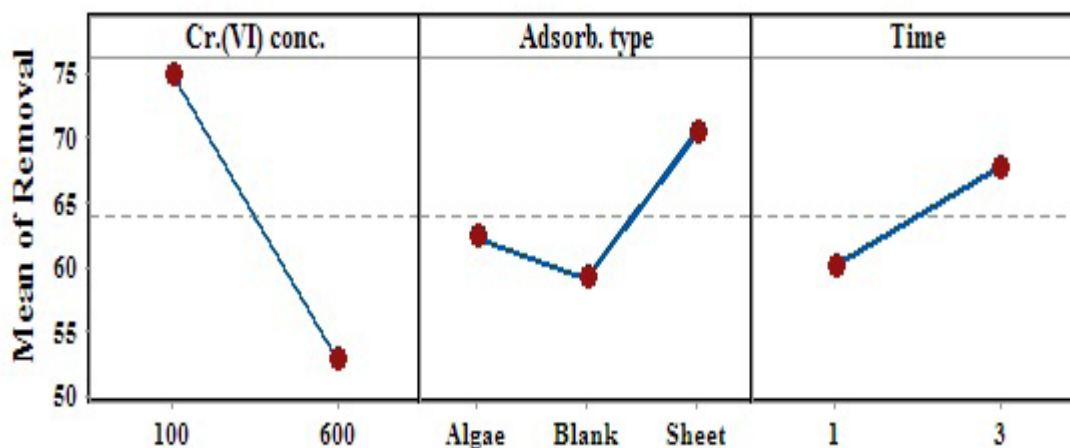


Fig. 5. Main effects plot for the CRE at low and high levels of each factor for the PAS.

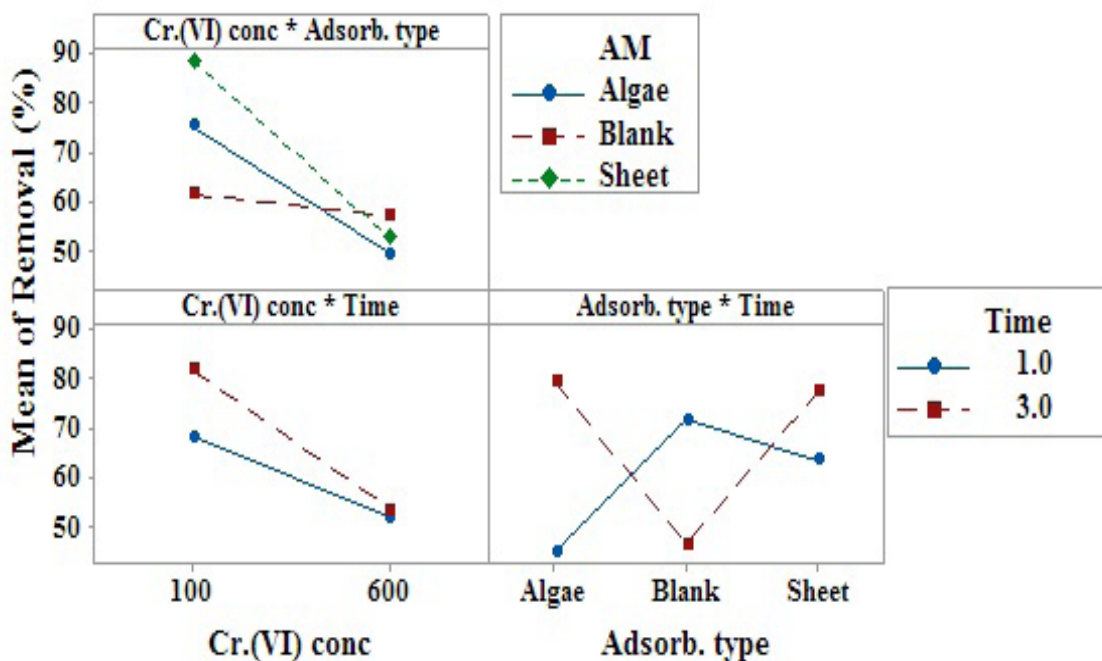


Fig. 6. Interaction effects plot for the CRE for the PAS.

Analysis of variance (ANOVA)

Analysis of variance (ANOVA) test was used in order to detect the significant factors that affecting the CRE. Data listed in Table 4 exhibited the sum of squares that used to determine the factors' effects and the F-ratios (F_0), the ratio of the respective mean-square effect and the mean-square error. Furthermore, P- Values that was

known as "the smallest level of significance leading to not-accepting the null hypothesis". It stated that the main and the interaction effects of each factor were statistically significant when $P < 0.05$. In this study, the effects (Cr (VI) 100 ppm and two way interaction effect "Adsorbent type with time") displayed the higher statistically significance effect, see Table (3).

TABLE 4. Analysis of variance for the Qe (mg/g) of the BM.

Source	DF	Adj SS	Adj MS	F-Value	P-Value
Main effects	4	3828.4	957.1	6.35	0.006
2-Way Interactions	5	4855.1	971.0	6.44	0.004
3-Way Interactions	2	1998.2	999.1	6.63	0.011
Cr (VI) conc.*Adsorb. type*Time	2	1998.2	999.1	6.63	0.011
Error	12	1808.3	150.7		
Total	23	12490.0			

Student's t-test

Student t-test express the pareto chart that resulted from the factorial design experiment where the Pareto chart showed the absolute values of the standardized main and interaction effects represented by horizontal columns from the largest effect (i.e. tallest column) to the smallest effect (i.e. shortest column). Student's t-test was displayed to determine if the calculated effects were significantly different from zero or not. It was noticed that for a 95% confidence level and twelve degree of freedom, the *t*-value was equal to 2.179. These results were illustrated in the pareto chart Fig (7) where the vertical line refers to the *t*-value of the CRE at 95% confidence level. "Values presented in the horizontal columns are Student's *t*-test values for each effect. The values that exceed the reference line are significant values" whereas the values that not exceed the line are non-significant values [26]. According to the reported pareto chart, the main effects (A) and the interaction effect (BD and ABD) that extend over the vertical line were significant. The Cr (VI) Concentration (A) exhibited the highest significant effect on the CRE followed by BD and ABD two and three way interactions ("Adsorbent type with time" and "Cr (VI) conc. with Adsorbent type, and time").

Response optimizer

Response optimizer (Fig 8) aimed to select the best parameters that allow obtaining the highest CRE. It considered a useful tool for prediction of multiple parameters on a response. In the current work, it was stated that the interaction between the following factors sheet adsorbent type at 100 ppm Cr (VI) for 3 h shaking achieve the highest Cr (VI) of 97.49 % with a degree of desirability 98.8.

Recovery and reuse of PAS

EDTA, HCl, NaOH and HNO₃ (0.1 M) were used in the desorption study (Cr recovery). It was observed that 90 % of the loaded chromium ions were desorbed with 0.1 M EDTA as previously reported. While 0.1 M of HCl, NaOH and HNO₃ were not effective in the desorption studies of chromium. The regenerated PAS after recovery process were successfully used three times adsorption-desorption cycles (see Table5). It was observed that the capacity of sheet was decreased with 30 % after the first cycle. Thus, these results emphasized on the PAS can be used in Cr. (VI) ions removal and repeated more than one time.

Langmuir and Freundlich isotherm:

Adsorption data were analyzed according to the two equations; Langmuir and Freundlich adsorption isotherm linear form. In Langmuir isotherm, a linear plot of the specific sorption (Ce/qe) against the equilibrium concentration (Ce) for the Cr (VI) removal by PAS was plotted. The Linear plot of Langmuir and Freundlich isotherms for the PAS were shown in Fig 9, 10. Furthermore, the calculated results of both models were displayed in Table 6. High R² value of Langmuir isotherm was exhibited fitting to the model of the adsorption process[27]. Thus, the results supposed that the process of adsorption was a monolayer[28]. Therefore, the nature of the adsorbent surface was homogenous. Once chromium occupies of the functional groups of the PAS, no further adsorption can take place on the surface and there is no further interaction between molecules adsorbed and neighboring sites [29].

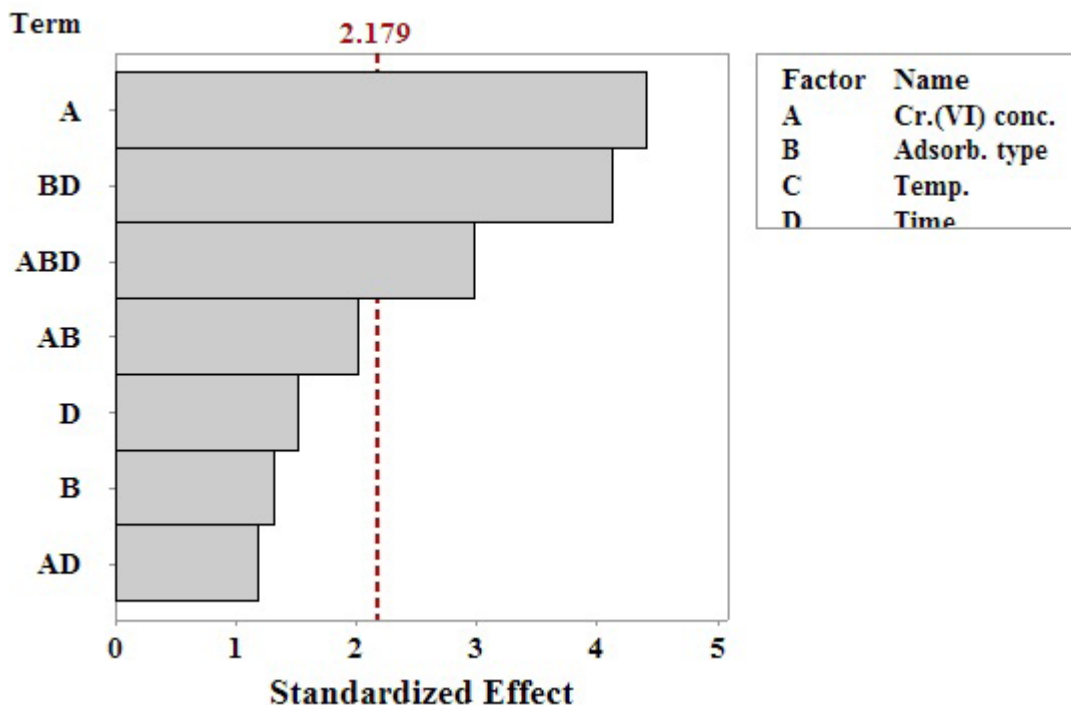


Fig. 7 . Pareto chart of the standardized main and interaction effects for the PAS.

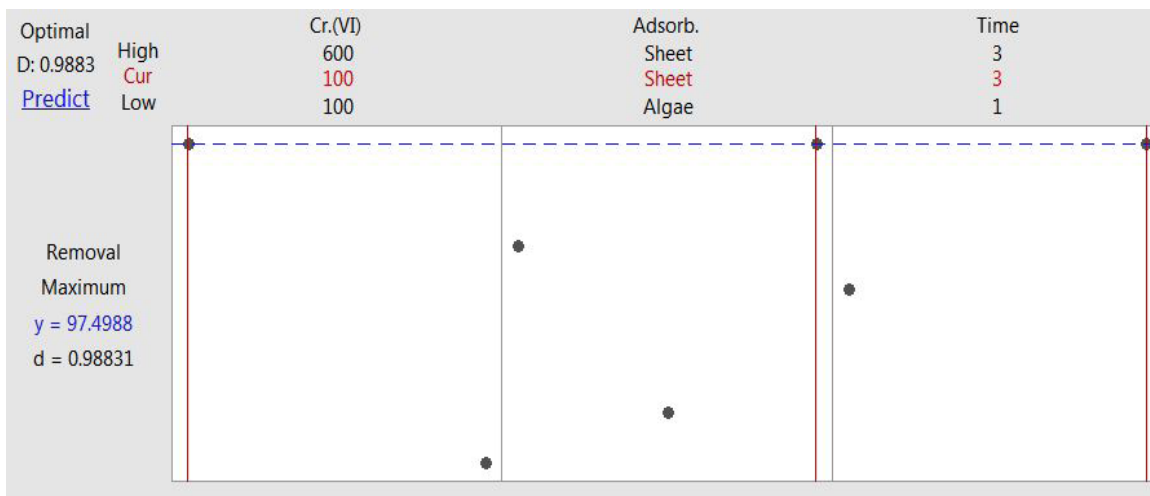


Fig.8 . The optimization plot displayed the fitted values for the predictor settings to maximize the CRE of for the PAS.

TABLE 5. Desorption study of chromium from polymer sheets.

Treat	Removal first run	Recovery %	Removal second run	Recovery %	Removal third run
Blank	42.67515924	90.29850746	28.39506173	97.82608696	13.38912134
*PAS 1	71.33757962	32.58928571	36.11111111	43.58974359	37.96296296
PAS 2	57.96178344	43.40659341	39.19753086	37.00787402	32.09876543

*PAS polymer algal sheet

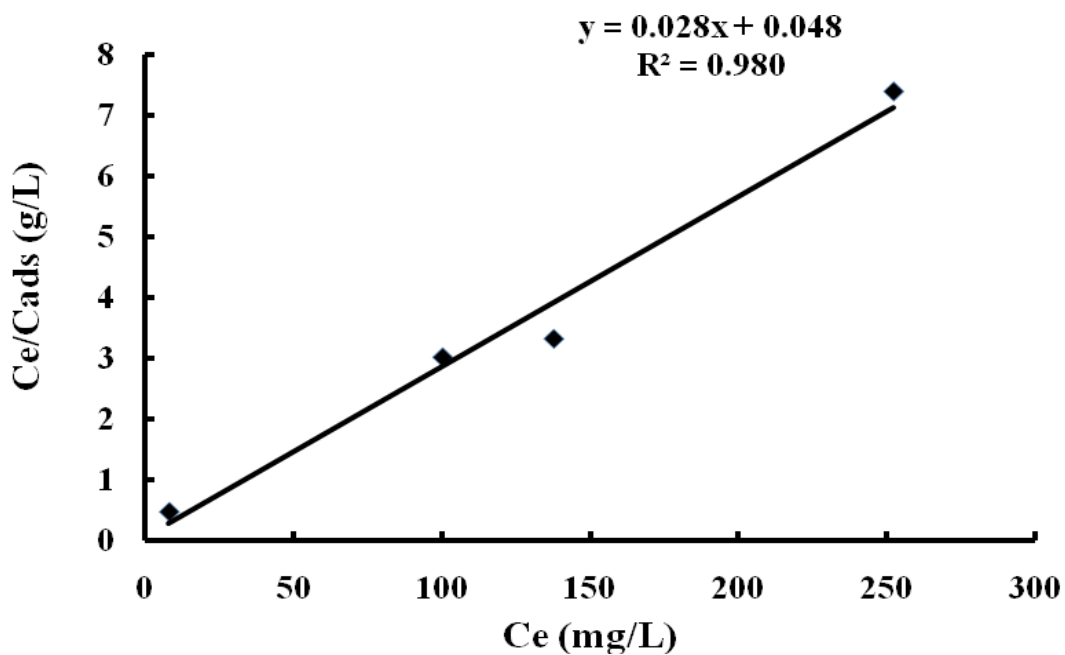


Fig.9 . Langmuir isotherm plot of the PAS.

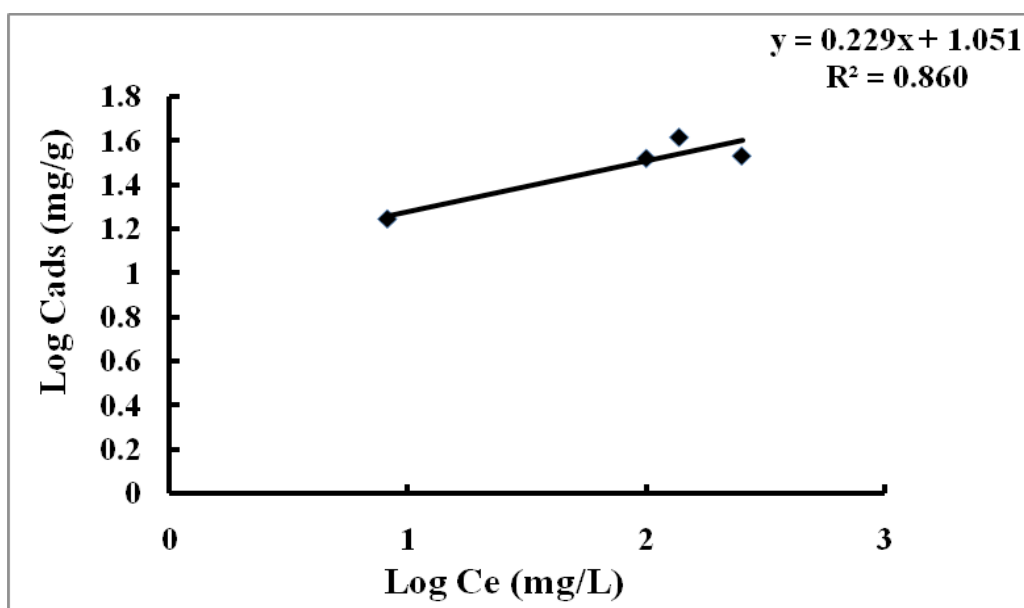


Fig.10. Freundlich isotherm plot of the PAS.

TABLE 6. Langmuir and freundlich Isotherm parameters for Chromium ions adsorbed by polymer and algae polymer sheets.

Model	Parameters	Parameters	R^2
Langmuir	Q_{max}	B	R^2
	35.71428571	736.377025	98.03
Freundlich	n	K_f	R^2
	4.351610096	11.26419085	86.06

*Sorption Kinetics:**Pseudo 1st order kinetics*

This equation described the adsorption in solid-liquid systems that depended on the sorption capacity of solids. Assumption of this equation suggests that the Cr (VI) ions are adsorbed on one site on the surface PAS or polymer separately [30,31].

The linear form of pseudo 1st order kinetics is

$$\log(q_e - qt) = \log q_e - \frac{k_1 t}{2.303} \dots\dots (5)$$

Where q_e and qt represented the amounts of adsorbed Cr (VI) on the adsorbent at equilibrium

and at time t , respectively (mg/g), and k_1 represented the first-order adsorption rate constant (min^{-1}).

In the present work, Fig. 11 showed the linear form of the pseudo-first-order model for the sorption of Cr (VI) ions on the PAS at Cr (VI) initial concentration 100 mg/l [32,33]. The calculated results of the first-order rate equation were displayed in Table (7) where the acquired q_e value by this method is not equal to the experimental value. Therefore, the reaction cannot be classified as pseudo-first-order reaction.

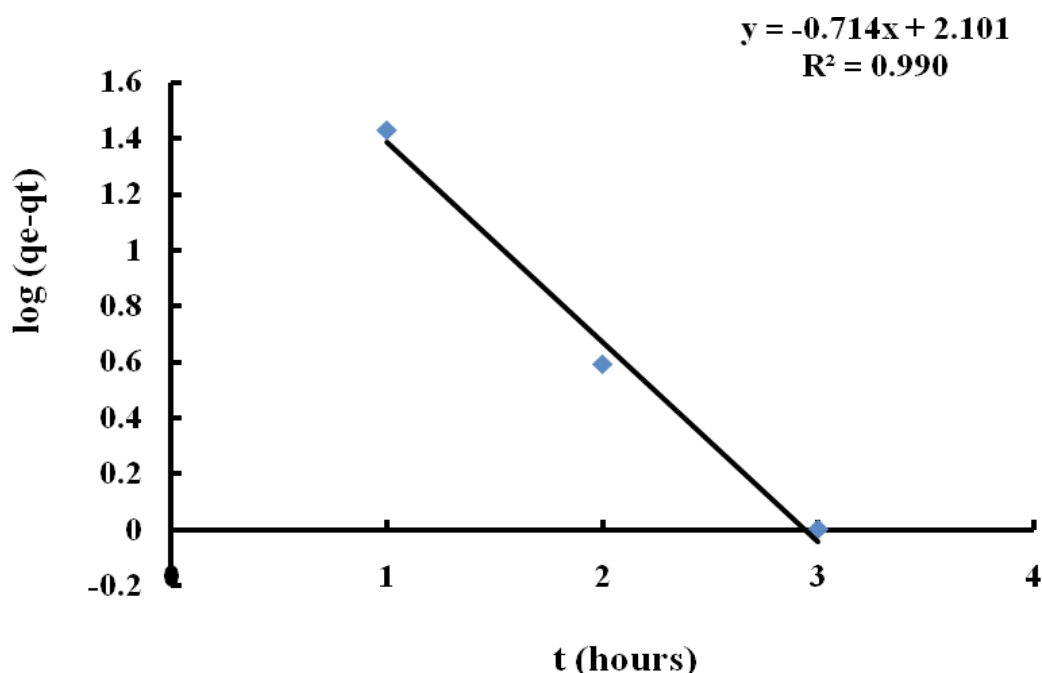


Fig. 11. Pseudo-first-order sorption kinetics of Cr (VI) onto the PAS (initial concentration: 100 mg/l, contact time: 1, 2, 3, 6, 24 hours, and agitation 100 rpm).

TABLE 7. Kinetic parameters for Cr (VI) adsorption by prepared magnetite nanoparticles (polymer and algae polymer sheet, pH value: 7, initial concentration: 100 mg/l, contact time: 1-24 h, and agitation speed: 100 rpm).

Model	Parameters			
	q_e calc.	$q_{e\text{exper}}$	K_1	R^2
Pseudo first order kinetics	126.3863	45.01505922	-1.6450329	99.01
Pseudo second order kinetics	q_e calc.	$q_{e\text{exper}}$	K_2	R^2
	50.76142132	45.01505922	0.021802809	99.66

Pseudo 2nd order kinetics

The equation of pseudo second order kinetic can be expressed as follow:

$$\frac{T}{qt} = \frac{1}{k_2 qe^2} + \frac{1}{qe} t \quad \dots\dots\dots (6)$$

Where K_2 , the pseudo-second-order rate constant of adsorption (gm/g min).

Linear plot of t/qt vs. t was achieved according to Eq. 6 (see Fig 12). The k and qe values were

calculated from the slope and intercept and were showed in Table 7. The correlation coefficients R^2 of the pseudo-second order equation for the linear plots of PAS was very close to 1 (nearly 99.66 %). Besides, the calculated qe values were agreed well with the experimental value. These results supported the assumption of this model “the rate limiting step in adsorption is chemisorption involving valence forces through the sharing or exchange of electrons between adsorbent and metal ions”.

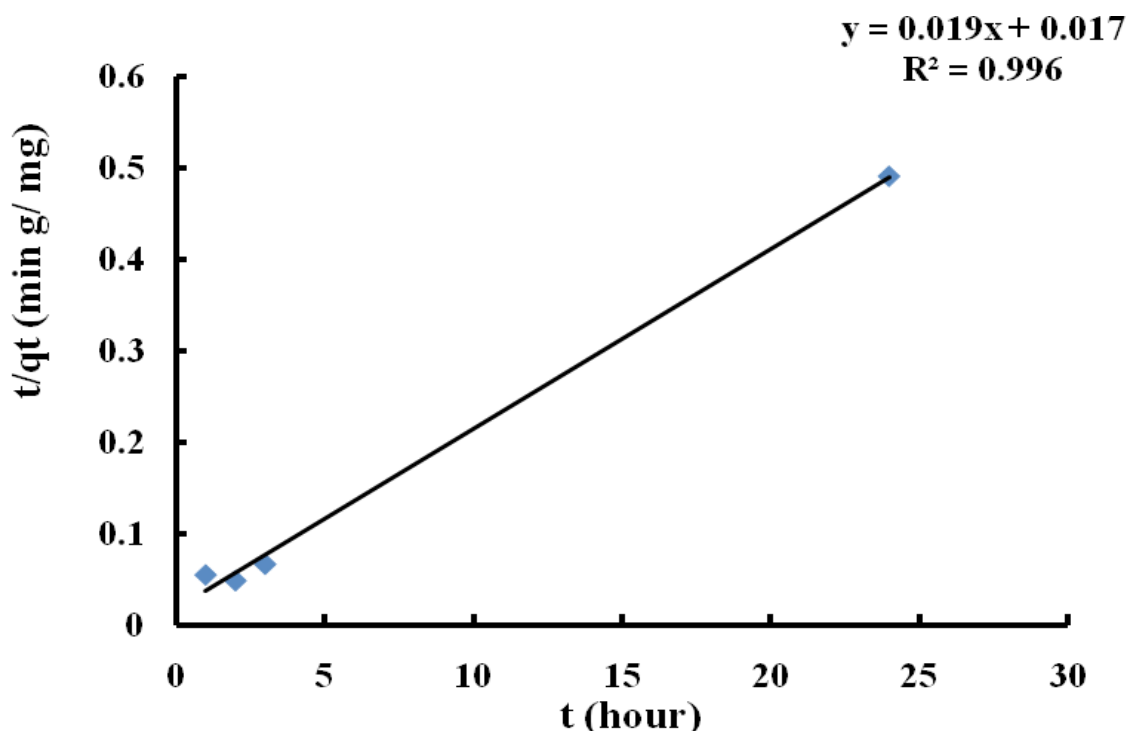


Fig.12. Pseudo-second-order sorption kinetics of Cr (VI) onto the PAS (initial concentration: 100 mg/l, contact time: 1, 2, 3, 6, 24 h, and agitation 100 rpm).

Conclusion

Polymer algae sheet (PAS) was a great solution for easier harvesting and dewatering of biomass after metal removal process. Polymerization of 0.3 g/ 100 ml solution Sargassum dentifolium algae with (PVA/MAA/HEMA) polymer material achieved 70% of chromium removal. Application of full factorial design experiments achieved the highest CRE of 98.41 % at 50° C, 100 ppm Cr (VI) solution after 3 hour shaking by using the PAS as a biosorbent material. From previous results, it can be concluded that using the PAS is an effective way

to obtain highest chromium removal efficiency in contrast to using polymer material and Sargassum dentifolium separately. Furthermore, 0.3 mg from polymerized Sargassum dentifolium was achieved the highest removal efficiency by comparing with other used doses. Moreover, EDTA was the best material that displayed the highest recovery value of 90 %. Furthermore, the PAS can be used until 3 times adsorption-desorption processes. Further work in the future can be displayed on the elasticity & hardness of the sheet and more optimization conditions for the percent of the biomass with polymer material.

References

1. Sheth, K. and V.M. Soni, Comparative study of removal of Cr (VI) with PAC, GAC and adsorbent prepared from tobacco stems. *JOURNAL OF INDUSTRIAL POLLUTION CONTROL.*, **20**(1),45-52(2004).
2. Wu, Y., et al., Adsorption of chromium (III) on lignin. *Bioresource technology*, **99**(16), 7709-7715(2008).
3. Samaras, P., et al., Effect of hexavalent chromium on the activated sludge process and on the sludge protozoan community. *Bioresource technology*, **100**(1), 38-43(2009).
4. Das, D.D., et al., Removal of Cr (VI) from aqueous solution using activated cow dung carbon. *Journal of Colloid and Interface Science*, **232**(2), 235-240(2000).
5. Kiran, M.G., K. Pakshirajan, and G. Das, Heavy metal removal from multicomponent system by sulfate reducing bacteria: mechanism and cell surface characterization. *Journal of hazardous materials*, **324**, 62-70(2017).
6. Huang, J., et al., Influence of pH on heavy metal speciation and removal from wastewater using micellar-enhanced ultrafiltration. *Chemosphere*, **173**, 199-206(2017).
7. Chen, Z., et al., Layered silicate RUB-15 for efficient removal of UO₂²⁺ and heavy metal ions by ion-exchange. *Environmental Science: Nano*, **4**(9),1851-1858(2017).
8. Bhusari, V., et al., Comparative study of removal of hexavalent chromium from water using metal oxide nanoparticles. *Advances in Nanoparticles*, **5**(01), 67(2016).
9. Baltazar, M.d.P.G., et al., Copper biosorption by *Rhodococcus erythropolis* isolated from the Sossego Mine–PA–Brazil. *Journal of Materials Research and Technology*, (2018).
10. Michalak, I., K. Chojnacka, and A. Witek-Krowiak, State of the Art for the Biosorption Process—a Review. *Applied Biochemistry and Biotechnology*, **170**(6), 1389-1416(2013).
11. Rao, P. and S. Bhavikatti, Removal of chromium (VI) from synthetic waste water using immobilized algae. *International Journal of Current Engineering and Technology*, (2013).
12. Sekomo, C.B., et al., Heavy metal removal in duckweed and algae ponds as a polishing step for textile wastewater treatment. *Ecological engineering*, **44**, 102-110(2012).
13. Bağda, E., A. Sarı, and M. Tuzen, Effective uranium biosorption by macrofungus (*Russula sanguinea*) from aqueous solution: equilibrium, thermodynamic and kinetic studies. *Journal of Radioanalytical and Nuclear Chemistry*, **317**(3), 1387-1397(2018).
14. Mechirackal Balan, B., et al., Mercury tolerance and biosorption in bacteria isolated from Ny-Ålesund, Svalbard, Arctic. *Journal of basic microbiology*, **58**(4), 286-295(2018).
15. Yen, H.-W., et al., The use of autotrophic *Chlorella vulgaris* in chromium (VI) reduction under different reduction conditions. *Journal of the Taiwan Institute of Chemical Engineers*, **74**, 1-6(2017).
16. Ardila, L., R. Godoy, and L. Montenegro. Sorption Capacity Measurement of *Chlorella Vulgaris* and *Scenedesmus Acutus* to Remove Chromium from Tannery Waste Water. in *IOP Conference Series: Earth and Environmental Science*. (2017). IOP Publishing.
17. Foroutan, R., R. Mohammadi, and B. Ramavandi, Treatment of chromium-laden aqueous solution using CaCl₂-modified *Sargassum oligocystum* biomass: Characteristics, equilibrium, kinetic, and thermodynamic studies. *Korean Journal of Chemical Engineering*, **35**(1), 234-245(2018).
18. Asnaoui, H., A. Laaziri, and M. Khalis, Biosorption of chromium (Cr) onto algae (*Ulva lactuca*): application of isotherm and kinetic models. *Moroccan Journal of Chemistry*, **5**(1), 5-1- 186-195 (2017).
19. Murphy, V., H. Hughes, and P. McLoughlin, Comparative study of chromium biosorption by red, green and brown seaweed biomass. *Chemosphere*, **70**(6), 1128-1134(2008).
20. Yodsuwan, N., et al., Ohmic heating pretreatment of algal slurry for production of biodiesel. *Journal of biotechnology*, **267**, 71-78(2018).
21. Kern, J.D., et al., Using life cycle assessment and techno-economic analysis in a real options framework to inform the design of algal biofuel production facilities. *Bioresource technology*, **225**, 418-428(2017).

22. Mallick, N., Biotechnological potential of immobilized algae for wastewater N, P and metal removal: a review. *biometals*, **15**(4), 377-390(2002).
23. Hedayatkah, A., et al., Bioremediation of chromium contaminated water by diatoms with concomitant lipid accumulation for biofuel production. *Journal of environmental management*, **227**, 313-320(2018).
24. Amarasinghe, B. and R. Williams, Tea waste as a low cost adsorbent for the removal of Cu and Pb from wastewater. *Chemical Engineering Journal*, **132**(1-3), 299-309(2007).
25. Mathialagan, T. and T. Viraraghavan, Biosorption of pentachlorophenol by fungal biomass from aqueous solutions: a factorial design analysis. *Environmental technology*, **26**(5), 571-580(2005).
26. Chang, C. and Y. Ku, The adsorption and desorption characteristics of EDTA-chelated copper ion by activated carbon. *Separation science and technology*, **30**(6), 899-915(1995).
27. Ho, Y.-S., W.-T. Chiu, and C.-C. Wang, Regression analysis for the sorption isotherms of basic dyes on sugarcane dust. *Bioresource technology*, **96**(11), 1285-1291(2005).
28. Saadi, R., et al., Monolayer and multilayer adsorption isotherm models for sorption from aqueous media. *Korean Journal of Chemical Engineering*, **32**(5), 787-799(2015).
29. Langmuir, I., I. Langmuir, *J. Am. Chem. Soc.*, **38**, 2221(1916).
30. Hao, Y.-M., C. Man, and Z.-B. Hu, Effective removal of Cu (II) ions from aqueous solution by amino-functionalized magnetic nanoparticles. *Journal of Hazardous Materials*, **184**(1-3), 392-399(2010).
31. Hu, X.-j., et al., Adsorption of chromium (VI) by ethylenediamine-modified cross-linked magnetic chitosan resin: isotherms, kinetics and thermodynamics. *Journal of hazardous materials*, **185**(1), 306-314(2011).
32. Yuh-Shan, H., Citation review of Lagergren kinetic rate equation on adsorption reactions. *Scientometrics*, **59**(1), 171-177(2004).
33. Lasheen, M., et al., Removal and recovery of Cr (VI) by magnetite nanoparticles. *Desalination and Water Treatment*, **52**(34-36), 6464-6473(2014).

البلمرة الإشعاعية لحمض عديد الفينيل / حمض المالك / هيم / طحلب السراجسسام لإزالة الكروم السداسي من محاليله المائية

طارق منصور محمد¹ ، احمد ابراهيم لينة² ، نبيله احمد مزيدا¹، شيماء حسين²

¹ هيئه الطاقة الذريه

² معهد بحوث البترول

تعتبر الطحالب البحريه ذات اهميه قصوى نظرا لطبيعه تركيبها وتوافرها ورخص سعرها وايضا كونها صديقه للبيئه ومن هذا المنطلق فقد تم في هذا البحث تحضير توليفه من طحلب السراجسسام مع حمض عديد الفينيل والهيم (2-هيدروكسي ايثيل ميثاكريلات) وحمض المالك على هيئه أغشيه باستخدام تكنولوجيا الاشعاع الجامي وذلك بهدف التخلص من أيونات عنصر الكروم كنموذج لبعض أنوية المواد السامه والثقله. وقد تم في هذا البحث دراسة الظروف المناسبه لعملية التحضير وتم توصيف الاغشيه المحضره باستخدام جهاز الاشعه تحت الحمراء وجهاز الميكروسكوب الماسح الالكتروني وجهاز حيود الاشعه السينيه. ومن الناحية التطبيقيه تم استخدام الاغشيه المحضره لامتراز عنصر الكروم السام من محاليله المائيه ودراسة العوامل التي تؤثر على عملية الامتصاص مثل الاس الهيدروجيني ودرجات الحراره وزمن التفاعل وكذلك تم دراسة الكيناتيكيه الحركيه للتفاعل وذلك بتطبيق معادله لانجمير التي أوضحت أن التفاعل من الدرجه الثانيه الزائفه وكذلك تم تطبيق معادله فرنشل التي وصفت الطبيعه الحركيه لعملية الامتراز وقد خلص البحث الى أن الاغشيه المحضره لها قدره عاليه على امتراز أيونات الكروم من محاليله المائيه .